JACS
JOURNAL OF THE AMERICAN CHEMICAL SOCIETY

Article

pubs.acs.org/JACS

Restricted State Selection in Fluorescent Protein Förster Resonance Energy Transfer

Thomas A. Masters,[†,‡,§] Richard J. Marsh,[†] Daven A. Armoogum,[†] Nick Nicolaou,[†] Banafshé Larijani,*[,‡] and Angus J. Bain*[,†]

[†]Department of Physics and Astronomy, University College London, Gower Street, London WC1E 6BT, United Kingdom

[‡]Cell Biophysics Laboratory, Cancer Research U.K., Lincoln's Inn Fields Laboratories, London Research Institute, London WC2A 3LY, United Kingdom

Supporting Information

ABSTRACT: The measurement of donor lifetime modification by Förster resonance energy transfer (FRET) is a widely used tool for detecting protein−protein interactions and protein conformation change. Such measurements can be compromised by the presence of a significant noninteracting fraction of molecules. Combining time-resolved intensity and anisotropy measurements gives access to both molecular distance and orientation. Fluorescent proteins frequently used to detect energy transfer in biological systems often exhibit decay characteristics indicative of more than one excited state. However, little attention has thus far been given to the specific modes of energy transfer, in particular, which states are predominantly coupled. Here, we use a previously characterized dimerization system to study energy transfer between EGFP and mCherry. Optically excited EGFP and mCherry both exhibit biexponential decays, and FRET should therefore involve dipole−dipole transfer between these four states. Analysis of the sensitized fluorescence anisotropy and intensity decays indicates that FRET transfer is predominantly from the shorter lived EGFP emitting state (2.43 ns) to the longer lived (ca. 2.77 ns) minority component (ca. 16%) of the optically excited mCherry emission. This high degree of state selection between these two widely used FRET pairs highlights the fundamental differences that can arise between direct optical excitation of an isotropic molecular population and dipole−dipole coupling in a far from isotropic interaction geometry and has consequences regarding the accurate interpretation of fluorescent protein FRET data.

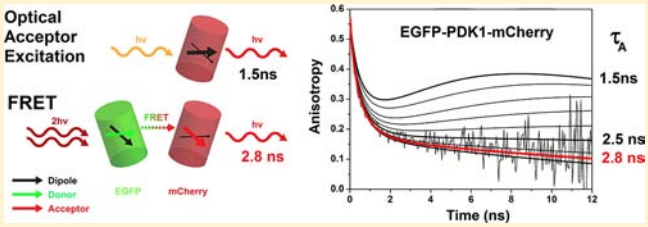

INTRODUCTION

FRET involves the nonradiative transfer of electronic energy between a closely spaced pair of donor and acceptor molecules. The rate at which energy is transferred from optically excited donors to acceptors is dependent on the inverse sixth-power of the donor−acceptor separation and the relative orientation of their transition dipole moments. Because of this sensitive distance-dependence, FRET has long been known as a spectroscopic ruler[1] and has become widely used to detect protein conformation change and intermolecular interactions.[2] The enhanced rate of de-excitation of donor molecules depends on the rate of energy transfer, and so the shortening of the donor lifetime is an indicator of this effect. Fluorescent proteins often exhibit decay characteristics indicative of more than one excited state; however, when making time-domain measurements, only a single decay component is often used to model the donor emission intensity due to low signal-to-noise. Extraction of the FRET rate from donor lifetime measurements is often prohibitively difficult, first, when investigating protein−protein interactions in which only a fraction of the total population interact; measurement of the donor lifetime in the presence of the acceptor will yield (at least) a biexponential decay. Extraction of the minority decay component (given the intrinsic donor lifetime) will yield the transfer rate. Signal-to-noise considerations often prevent the identification of this decay component particularly when only a small subset of donors undergoes FRET. In recent work,[3] we demonstrated that the FRET rate in such a system can be determined by analysis of the time-resolved emission intensity of the FRET acceptor. As a result of FRET, a growth is apparent in the acceptor emission at a rate equal to that of the decay rate of the donor in the presence of the acceptor.[4] This phenomenon has previously been used to characterize the transfer of energy from the tryptophan residue to the chromophore of various fluorescent proteins[5] and to study the conformation of a calcium sensor.[6] In the analysis of time-resolved fluorescence data, a growth in fluorescence corresponds to a negative pre-exponential factor,[7] which is easily identifiable from (positive) spontaneous emission decay components arising from non-interacting donor emission and direct acceptor excitation. These latter components may be large if only a small fraction of molecules undergo FRET. It is well-known that the anisotropy of sensitized acceptor emission can in principle be used to determine the donor−acceptor transition dipole moment angle setting limits on the FRET orientation factor κ^2,[8] thus allowing

Received: December 14, 2012
Published: April 18, 2013

 © 2013 American Chemical Society dx.doi.org/10.1021/ja312230b | J. Am. Chem. Soc. 2013, 135, 7883−7890

a more accurate determination of the donor−acceptor distance.[9,10] In partially interacting systems, the sensitized acceptor anisotropy decay comprises a time-dependent (population) weighted sum of the intrinsic anisotropies of the excited states of both interacting and noninteracting donors and acceptors. The surprising usefulness of this apparent complexity in the fluorescence anisotropy in analyzing resonance energy transfer has hitherto not been recognized; the interplay between populations with different intrinsic anisotropy decays and fluorescence lifetimes gives rise to signatures that are strongly lifetime dependent and markedly different from those associated with rotational diffusion.[11−14]

In this Article, we employ the in vitro 3-Phosphoinositide Dependent Protein Kinase 1 (PDK1) dimerization system[6] to study state selection using time-resolved intensity and anisotropy measurements. We use two-photon excitation of the EGFP donor as it has several advantages for this purpose over our previous single-photon work.[3] The degree of direct acceptor (mCherry) excitation is greatly reduced, and the higher degree of angular photoselection afforded by two-photon excitation provides a greater dynamic range and sensitivity for FRET depolarization measurements. The composite fluorescence anisotropy from noninteracting donor emission and FRET excited acceptors is highly sensitive to any differences between the decay dynamics of the two populations. Through a combined analysis of sensitized donor intensity and anisotropy decays, we are able to conclude that in stark contrast to direct optical excitation, FRET transfer takes place predominantly to the longer lived (2.77 ns vs 1.47 ns) but minority decay component (ca. 16%) of mCherry.

Theory of Time-Resolved Fluorescence Intensity and Anisotropy in Systems Undergoing FRET. *Fluorescence Intensity.* With equal ground-state donor and acceptor populations and an interacting fraction F_I, following eqs SI-1−SI-5 in the Supporting Information, the intensity of fluorescence at time t after short pulsed excitation is given by:

$$I(t) \propto \exp(-(k_{FRET} + k_F^{DI})t)F_I[1 - BX] + BF_IX\exp(-k_F^{AI}t) + (1 - F_I)\exp(-k_F^{DNI}t) + B\frac{\sigma_2^A}{\sigma_2^D}\exp(-k_F^{ANI}t) \quad (1)$$

$$B = k_R^A q_A / k_R^D q_D \quad \text{and} \quad \delta = \sigma_2^A/\sigma_2^D \quad (2)$$

$$X = \frac{k_{FRET}}{k_{FRET} + k_F^{DI} - k_F^{AI}} \quad (3)$$

where k_{FRET} is the FRET rate, k_F^{DI} and k_F^{AI}, and k_F^{DNI} and k_F^{ANI} are the fluorescence decay rates for interacting and non-interacting donors and acceptors, k_R^D and k_R^A are the radiative rates of the donor and acceptors, respectively, q_A and q_D are the fractions of donor and acceptor emission that are observed in the selected wavelength range of the detection system, and σ_2^A and σ_2^D are the acceptor and donor two-photon action cross sections at the donor excitation wavelength. The first two terms in eq 1 are the fluorescence signal arising from the FRET interaction between the donor and acceptor; the remaining terms correspond to fluorescence arising from the decay of noninteracting donors and direct two-photon excitation of the acceptor.

A detection window in which the donor emission predominates ($B \cong 0$) will have a fluorescence intensity of the form:

$$I(t) \propto \exp(-(k_{FRET} + k_F^{DI})t)F_I + (1 - F_I)\exp(-k_F^{DNI}t) \quad (4)$$

Given a small F_I, this will be dominated by emission from noninteracting donors, and a biexponential decay will not necessarily be observed.[3] As discussed above, a direct measurement of the FRET rate by this approach is not possible. Selection of a detection window such that $BX > 1$ will yield a fluorescence signal with a rise due to FRET transfer to and emission from the acceptor. This will in general include a measurable bleed through of noninteracting donor emission, and, where unavoidable, emission from direct acceptor excitation and a multiexponential decay (eq 1) will be observed. The magnitude of the amplitude of the rise time to those of the decay components is given by:

$$|A_{RISE}| = \frac{F_I(BX - 1)}{(1 - F_I) + B(F_IX + \delta)} \quad (5)$$

This can be rearranged to determine F_I:

$$F_I = \left(\frac{|A_{RISE}|}{1 - |A_{RISE}|}\right)\left(\frac{1 + B\delta}{BX - 1}\right) \quad (6)$$

Fluorescence Anisotropy. In a heterogeneous population of species i with lifetimes τ_i and anisotropy decays $R_i(t)$, the composite fluorescence anisotropy is given by:[11−14]

$$R(t) = \sum_i W_i(t)R_i(t) \quad (7)$$

where $W_i(t)$ is the time-dependent weighting factor of component i. The initial fluorescence anisotropies of EGFP and mCherry are close to the theoretical value of 4/7, a single element transition tensor with a corresponding parallel emission transition dipole moment.[17,18] When FRET is substantially faster than reorientation, the application of eq 1 to eq 7 (see eqs S1-7−SI-10) yields:

$$R(t) = \frac{4}{7}\frac{\begin{pmatrix}\exp(-(k_{FRET} + k_F^A)t) \times \\ F_I\left(1 - \frac{BX}{2}(3\cos^2\theta_{DA} - 1)\right)A_I(t) \\ + F_IBX\exp(-k_F^At)\frac{1}{2}(3\cos^2\theta_{DA} - 1)A_I(t) \\ + (1 - F_I)\exp(-k_F^Dt)A_{NI}(t) \\ + B\delta A_{NI}(t)\exp(-k_F^At)\end{pmatrix}}{\begin{pmatrix}F_I(1 - BX)\exp(-(k_{FRET} + k_F^A)t) \\ + F_IBX\exp(-k_F^At) \\ + (1 - F_I)\exp(-k_F^Dt) + B\delta\exp(-k_F^At)\end{pmatrix}} \quad (8)$$

where θ_{DA} is the angle between the donor and acceptor transition dipole moments. The orientational relaxation of EGFP and mCherry can be taken as equivalent (see Supporting Information Appendix 5) giving common intrinsic orientational relaxation functions $A_I(t)$ and $A_{NI}(t)$ in the interacting and noninteracting fractions, respectively. Given slow rotational diffusion, the evolution of $R(t)$ is critically dependent on the

dx.doi.org/10.1021/ja312230b | J. Am. Chem. Soc. 2013, 135, 7883−7890

contribution of the interacting and noninteracting fluorescent populations. If the acceptor population has a shorter lifetime than that of the noninteracting donors, then the FRET depolarization due to θ_{DA} will be transient, giving a dip-and-rise in the fluorescence anisotropy that is characteristic of a heterogeneous population with unequal fluorescence decay rates and constituent anisotropies.[11−14]

MATERIALS AND METHODS

In Vitro Fluorescence of PDK1 Constructs. The preparation of pure EGFP and mCherry labeled recombinant PDK1 has been described in detail earlier.[3] In addition, samples of recombinant mCherry and EGFP were obtained commercially (Cambridge Biosciences). All samples were prepared in the same buffer as used for size exclusion chromatography[3] at a concentration of 1−10 μM in a quartz cuvette (Hellma). Absorption spectra were measured using a UV−vis spectrometer (Agilent 8453). Steady-state fluorescence emission and excitation spectra were recorded using a UV−visible fluorometer (Quanta Master PTI). To avoid concentration-dependent depolarization effects in time-resolved experiments, which can arise due to the large degree of overlap of donor (EGFP) emission and acceptor (mCherry) absorption spectra, acceptor emission anisotropy experiments were performed at 1−2 μM concentration.

A two-photon excitation wavelength of 880 nm was chosen for direct excitation of EGFP; here, the two-photon action cross sections of mCherry and EGFP are approximately 0.1 and 37 GM, respectively,[15,16] δ is minimized at ca. 2.70×10^{-3}, and the contribution of direct acceptor excitation to the observed fluorescence is approximately an order of magnitude lower than for single-photon excitation. Investigation of mCherry photophysics in the region of spectral overlap with that of EGFP required excitation wavelengths between 470 and 610 nm. These measurements were undertaken using pure recombinant mCherry or PDK1-mCherry constructs (as above). Sample excitation was achieved using two laser systems, a 76 MHz modelocked Ti:Sapphire oscillator (Mira900F, Coherent) pumped at 532 nm by a Nd:YVO_4 laser (Verdi V-10, Coherent), and the output of a regeneratively amplified Ti:Sapphire pumped tunable optical parametric amplifier OPA (Mira OPA, Coherent), delivering 200−250 fs pulses at a repetition rate of 250 kHz. The first system was used for both single- and two-photon excitation of EGFP and the latter for single-photon excitation of mCherry. For two-photon excitation of EGFP, a 4 MHz pulse train at 880 nm was produced by passing the 76 MHz Ti:Sapphire output through an acousto-optic modulator (Pulse select, APE); for single-photon excitation of EGFP, this was frequency doubled to 440 nm using a BBO crystal (Photox). Direct (selective) single-photon excitation of mCherry was achieved using the output of the OPA with a tuning range of 470−700 nm. For single-photon excitation, on-sample powers ranged between 0.3 and 1 μW, while the corresponding two-photon power range was between 3 and 4 mW.

To characterize the states involved in energy transfer, fluorescence intensity decays were recorded in two spectral windows spanning 520−542 nm (dominated by EGFP emission and so termed the donor window) and 630−650 nm (termed the acceptor window, but containing significant noninteracting donor bleed through; see Appendices 2 and 3 in the Supporting Information). Respectively, these used a 532 ± 11 nm bandpass filter (Chroma) and a combination of long- and short-pass filters (LS-650 short-pass and RG-630 long-pass filters, Corion). The donor and acceptor window values of B (eq 1) are 0 and ca. 20 (see Appendix 1 and Figure S1, Supporting Information). All experiments employed linearly polarized excitation with fluorescence collected in a 90° geometry using a 5 cm focal length lens (Melles Griot), spectrally filtered (as above) and detected by means of a microchannel plate photomultiplier (R3809U, Hamamatsu) coupled to a NIM-based TCSPC system (Ortec). Intensity decays were obtained using a linear polarizer set at 54.7° to the excitation polarization. For anisotropy decays, fluorescence emission polarized parallel and perpendicular to the excitation polarization and was collected sequentially (with 10 s intervals) using a rotating polarizer. Fluorescence intensity decays were fitted to a multiexponential model.[3] To extract rise times in the acceptor fluorescence decays, the data were deconvoluted with the instrument response function (68 ps fwhm) and χ_R^2 minimized by a Levenberg−Marquardt routine using FluoFit (PicoQuant GmBH).

RESULTS AND DISCUSSION

FRET Is Limited to Particular States of EGFP and mCherry. The PDK1 dimerization system comprises a set of constructs, which are known to dimerize in vitro,[3] EGFP-PDK1, PDK1-mCherry, and EGFP-PDK1-mCherry. An equimolar mixture of EGFP-PDK1 + PDK1-mCherry displays FRET dynamics similar to that of EGFP-PDK1-mCherry (a construct with no intramolecular transfer). The intensity decays (Figure 1a) were analyzed by deconvolution with the instrument response function (e.g., Figure 1b and c) and tail-fitting; the results are displayed in Table 1. FRET is most readily detected by observation of the growth in sensitized acceptor fluorescence in the acceptor window. It is evident that a rise in acceptor fluorescence is only observed in EGFP-PDK1-mCherry and the EGFP-PDK1 + PDK1-mCherry mixture. A 1 μM equimolar mixture of EGFP and mCherry shows no rise in acceptor fluorescence (not shown). This rapid (sub-ns) growth can only be due to resonance energy transfer. To obtain the time constant of this growth ($(k_{FRET} + k^I_D)^{-1}$), the decay was deconvoluted with the instrument response function. The results are shown in Table 1. The rapid growth, with rise times of 0.609 ns (EGFP-PDK1-mCherry) and 0.799 ns (EGFP-PDK1+PDK1-mCherry), is not observed in the decay of EGFP in the donor window of either construct. The intrinsic fluorescence decay of EGFP decay is biexponential;[19−21] when bound to PDK1 approximately equally weighted lifetimes of ca. 3.07 and 2.4 ns are found in the donor window with an average lifetime of 2.75 ns as observed for single-photon excitation.[3] The existence of two emitting populations in the excited state of EGFP has been ascribed to ground-state heterogeneity.[19] Analysis of the donor window decays in the EGFP-PDK1/PDK1-mCherry mixture and of EGFP-PDK1-mCherry exhibits biexponential behavior and shows evidence of FRET through a decrease in the average lifetime (2.50 and 2.61 ns, respectively) from that of EGFP-PDK1 (2.75 ns). These observations together with the lack of a slow rise component in the sensitized acceptor intensity are consistent with intermolecular as opposed to intramolecular energy transfer occurring in a subset of the total population of excited states arising from the partial association (dimerization) of PDK1.[3]

The two observed excited states of EGFP (GP, 520−542 nm, Table 1) are not equally affected by FRET. During transfer, the ca. 3 ns decay shows a small decrease in lifetime and becomes the majority component, while the faster (2.43 ns) decay is appreciably shortened (to 1.7 ns). This indicates that FRET transfer is largely restricted to the shorter lived excited state of EGFP. In either FRET system (EGFP-PDK1-mCherry or the EGFP-PDK1/PDK1-mCherry mixture), emission detected in the acceptor window following excitation of EGFP contains both sensitized acceptor emission and bleed-through from EGFP. The combined decay of these two components is experimentally described by single time constants of 2.591 ns (EGFP-PDK1-mCherry) and 2.617 ns (EGFP-PDK1+PDK1-mCherry). This is in contrast to the multiexponential decay that is predicted by eq 3. Both of these times are significantly longer than the average decay time for directly excited mCherry (clearly visible from Figure 1). The interacting fraction can be

dx.doi.org/10.1021/ja312230b | J. Am. Chem. Soc. 2013, 135, 7883−7890

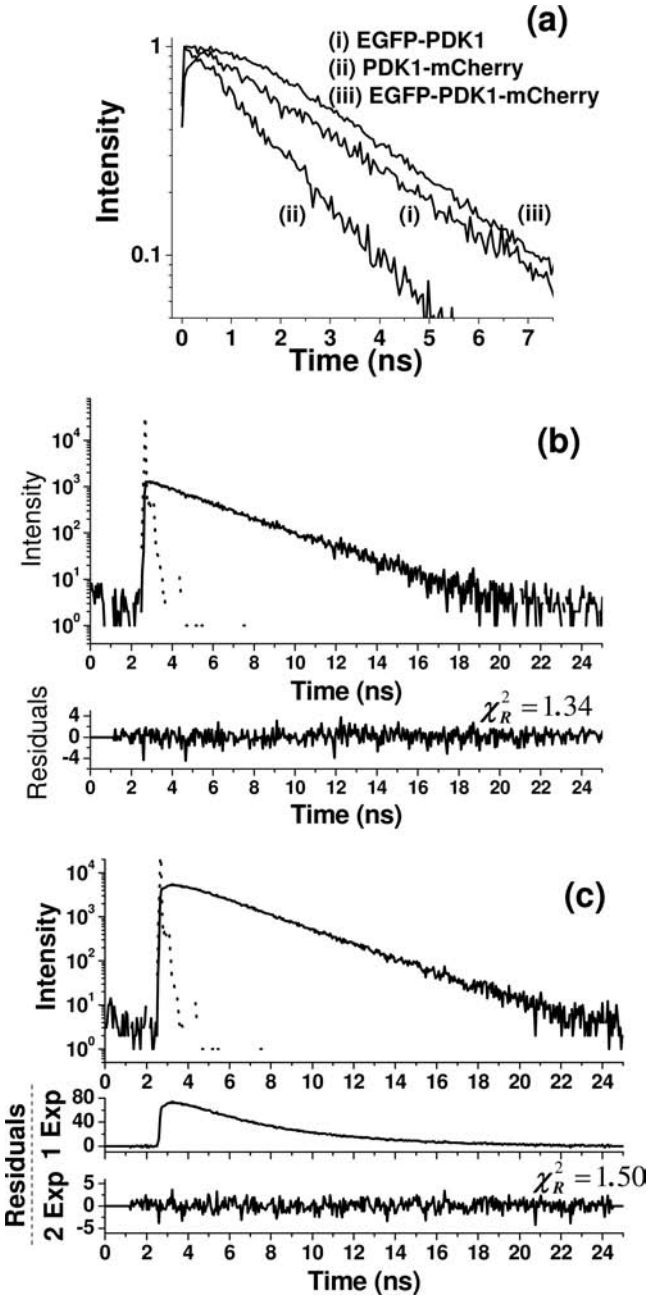

Figure 1. Acceptor window emission (630−650 nm) following two-photon excitation at 880 nm. (a) Comparison of the emission characteristics of (i) EGFP-PDK1, (ii) PDK1-mCherry, and (iii) EGFP-PDK1-mCherry. Deconvolution of the fluorescence decays (solid lines) with the instrument response function (dotted line) for (b) EGFP-PDK1 representative of noninteracting donor bleed through (i.e., no FRET) and (c) EGFP-PDK1-mCherry-sensitized mCherry fluorescence and noninteracting EGFP donor bleed through. The in-growth of mCherry emission following FRET is clearly visible in (a) (iii) and in (c) where the residual analysis clearly shows biexponential kinetics.

determined from eq 6, $|A_{RISE}|$, B, and δ are known; however, X depends on the acceptor lifetime through eq 3. The variation of F_I (and X) with acceptor lifetime (see Appendix 3 in the Supporting Information) is not large. For EGFP-PDK1-mCherry, given a rise-time of 0.609 ns with $|A_{RISE}| = 0.523 \pm 0.14$ and an interacting donor lifetime of 2.43 ns, F_I is in the region of 5−6% (see Figure S2). The calculated FRET amplitude to total detected signal was ca. 55% (see Figure S2). This together with the measured decay times strongly suggests that FRET excited mCherry emits with a longer effective lifetime than with optical excitation (see Figure 1a(ii)). If the FRET decay time is close to that of the donor bleed through (2.738 ns) and both signals have roughly equivalent weight, the two decay times are not easily resolvable.

From eq 8, $R(t)$ critically depends on the relative decay rates of the highly polarized noninteracting background (EGFP bleed through) and the FRET excited mCherry population whose anisotropy is considerably modified following transfer. Thus, we employed time-resolved fluorescence anisotropy measurements to determine the nature of the states in mCherry that were excited by dipole−dipole transfer.

Dipole−Dipole Transfer and Optical Excitation Access Different States of mCherry. The fluorescence anisotropy in the donor window following two-photon excitation of EGFP for EGFP-PDK1-mCherry, EGFP-PDK1+PDK1-mCherry, and EGFP-PDK1 is shown in Figure 3. Both FRET constructs show a rapid decrease in fluorescence anisotropy on a time scale similar to that of the in-growth of sensitized acceptor fluorescence. This is in sharp contrast to the anisotropy of EGFP-PDK1, which exhibits consistently higher anisotropy with a slow decay due to rotational diffusion (Table S1 and Figure S5, Supporting Information). The degree of fast depolarization in EGFP-PDK1 + PDK1-mCherry is lower than that for EGFP-PDK1-mCherry; in the double tagged construct, the dimeric association of PDK1 gives twice the probability of FRET transfer to mCherry than in EGFP-PDK1+PDK1-mCherry, and the effective interacting fraction (given equal donor and acceptor concentrations) is thus higher by this amount. The anisotropy dynamics are surprising. Depolarization of the acceptor emission due to FRET is well understood and expected;[3,4,9,10] however, the retention of low anisotropy in a heterogeneous population of interacting and noninteracting species is unexpected given the significantly shorter average lifetime of optically excited mCherry as compared to that of EGFP[3] (Table 1). The FRET excited mCherry population should be expected to decay significantly faster than that of the two-photon excited noninteracting EGFP population. As a result, the anisotropy should exhibit a dip and rise as the slower rotationally diffusing EGFP anisotropy predominates at longer times. From the analysis of the intensity data, it is clear that only one state in EGFP is participating in FRET, and the longer than expected decay of the acceptor window intensity indicates that the lifetime of the FRET excited population is longer than that accessed by direct optical excitation. While dipole−dipole transfer and single-photon excitation obey the same selection rules,[7,22] FRET takes place through energetically matched instantaneous donor de-excitations and acceptor excitations. The energy range of these transitions is determined by the overlap of the donor emission and acceptor absorption spectra. The overlap for EGFP and mCherry is shown in Figure 3. This is peaked to the blue of the mCherry optical absorption maximum of ca. 590 nm. If optical excitation and dipole−dipole transfer are equivalent, then an overlap-weighted average of the excited state decays accessed by single-photon excitation of mCherry across this window (shown in Figure 4) should yield the same decay dynamics as FRET excited mCherry. This gives two decay components with lifetimes of 1.47 and 2.77 ns with relative amplitudes of 0.844 (A_1) and 0.156 (A_2), respectively, corresponding to an average decay time of ca. 1.67 ns. Thus,

dx.doi.org/10.1021/ja312230b | J. Am. Chem. Soc. 2013, 135, 7883−7890

Table 1. Fitted Intensity Parameters Following Two-Photon Excitation of Fluorescent Protein Labeled PDK1 Samples[a]

	λ_{DET} (nm)	A_1	τ_1 (ns)	A_2	τ_2 (ns)	$\langle\tau\rangle$ (ns)
GP	520−542	0.503 ± 0.173	3.067 ± 0.11	0.497 ± 0.172	2.43 ± 0.12	2.75
GP+PC	520−542	0.579 ± 0.084	3.009 ± 0.055	0.421 ± 0.083	2.253 ± 0.081	2.69
GPC	520−542	0.728 ± 0.015	2.802 ± 0.011	0.272 ± 0.014	1.695 ± 0.037	2.50
GP	630−650	1.000 ± 0.014	2.738 ± 0.029	N/A	N/A	N/A
GP+PC	630−650	1.000 ± 0.006	2.617 ± 0.021	−0.190 ± 0.015	0.799 ± 0.122	N/A
PC	630−650	0.471 ± 0.024	1.156 ± 0.037	0.529 ± 0.015	1.942 ± 0.053	1.57
GPC	630−650	1.000 ± 0.010	2.591 ± 0.010	−0.523 ± 0.014	0.609 ± 0.022	N/A

[a]Abbreviations: EGFP-PDK1 (GP), PDK1-mCherry (PC), and EGFP-PDK1-mCherry (GPC). For GP+PC and GPC, the negative value of A_2 corresponds to the magnitude of the sensitized acceptor fluorescence, $|A_2| = |A_{RISE}|$, as in eqs 5 and 6.

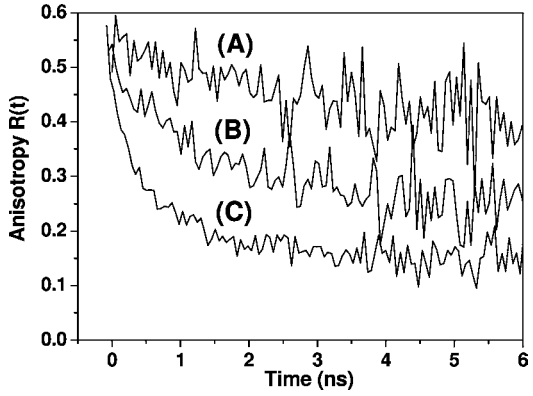

Figure 2. Acceptor window (630−650 nm) anisotropy decays following two-photon excitation at 880 nm. Comparison of (A) EGFP-PDK1 (no FRET), (B) EGFP-PDK1 and PDK1-mCherry, and (C) EGFP-PDK1-mCherry.

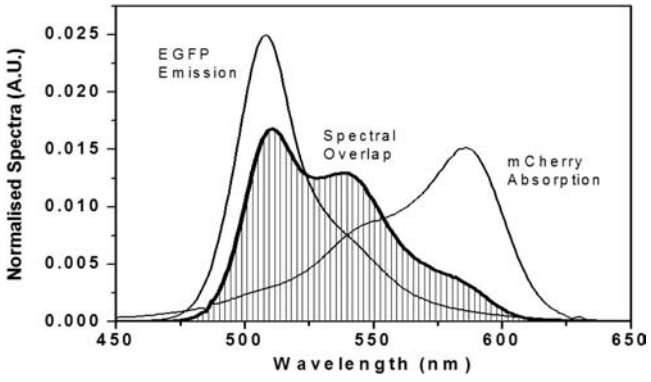

Figure 3. EGFP emission and mCherry absorption spectral overlap; FRET between EGFP and mCherry corresponds to single-photon excitation of mCherry at wavelengths predominantly to the absorption maximum of mCherry.

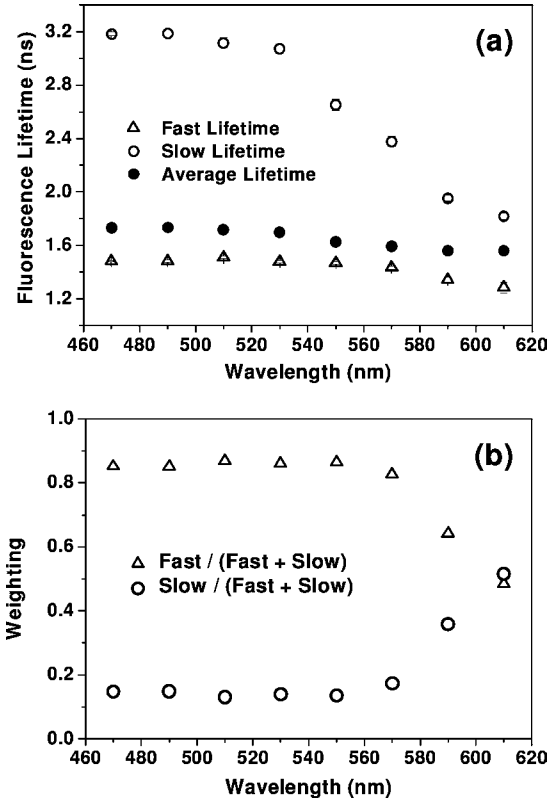

Figure 4. Variation in the acceptor window biexponential fluorescence decay characteristics of single-photon excited mCherry with excitation wavelength across the FRET excitation window of Figure 3.

optical excitation results in emission with predominantly faster overall decay kinetics than that observed following FRET. Model anisotropy decays for EGFP-PDK1-mCherry were generated using a modified form of eq 8. (See eq SI-30 in the Supporting Information.) Three examples corresponding to the equivalence between FRET and optical excitation are shown in Figure 5 with (A) a common interchromophore transition dipole moment angle for the short (1) and longer lived (2) states ($\theta_{DA1} = \theta_{DA2}$), (B) no FRET depolarization in transfer to the shorter lived state ($\theta_{DA1} = 0°$) with $\theta_{DA2} = 20°-90°$, and (C) maximum depolarization in FRET to the longer lived state $\theta_{DA2} = 90°, \theta_{DA1} = 0-90°$. In all of these cases, it is impossible to reproduce the experimentally observed anisotropy decay. The composite anisotropy either contains a dip and rise due to the shorter 1.47 ns lifetime or fails to produce the degree of fast depolarization due to the lower contribution of the longer lived (2.77 ns) state. The amplitudes of the two populations in mCherry that are excited by single-photon photoselection cannot be present in the FRET-induced emission. An anisotropy decay that contains the necessary degree of FRET depolarization without a subsequent rise is only possible where emission from the longer lived state of mCherry predominates. The anisotropy arising from FRET to a single excited state population with a variable lifetime is shown in Figure 6a where the sensitivity of the composite anisotropy to the difference between the lifetimes of the FRET excited population and the noninteracting donor background is clearly demonstrated. The lack of a rise in the anisotropy can only be achieved for an mCherry lifetime that can be no shorter than ca. 200 ps of the noninteracting EGFP background (2.738 ns Figure 1b and Table 1). Anisotropy decays corresponding to

dx.doi.org/10.1021/ja312230b | J. Am. Chem. Soc. 2013, 135, 7883−7890

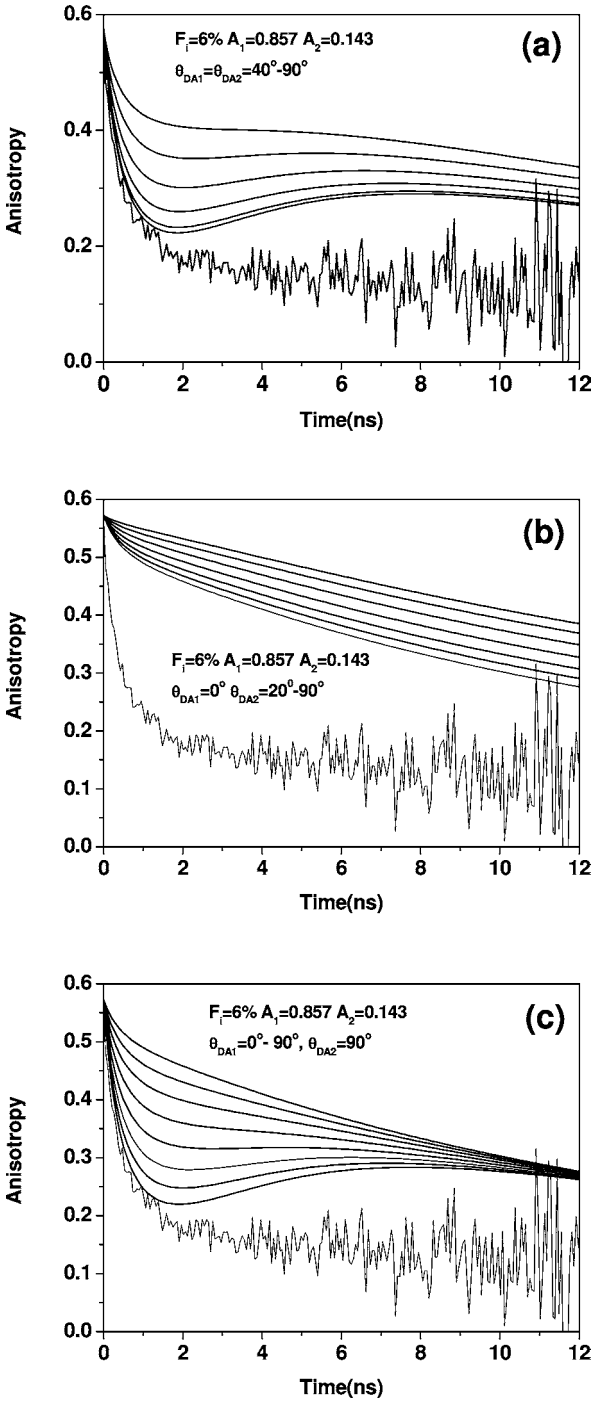

Figure 5. Model acceptor window anisotropy decays for EGFP-PDK1-mCherry assuming the equivalence of dipole−dipole state selection and direct optical excitation. (a) Equivalent interchromophore transition dipole moment angles, (b) no depolarization in FRET to the short-lived state, variable FRET depolarization to the long-lived state, and (c) maximum depolarization in FRET to the long-lived state, variable depolarization in FRET to the short-lived state.

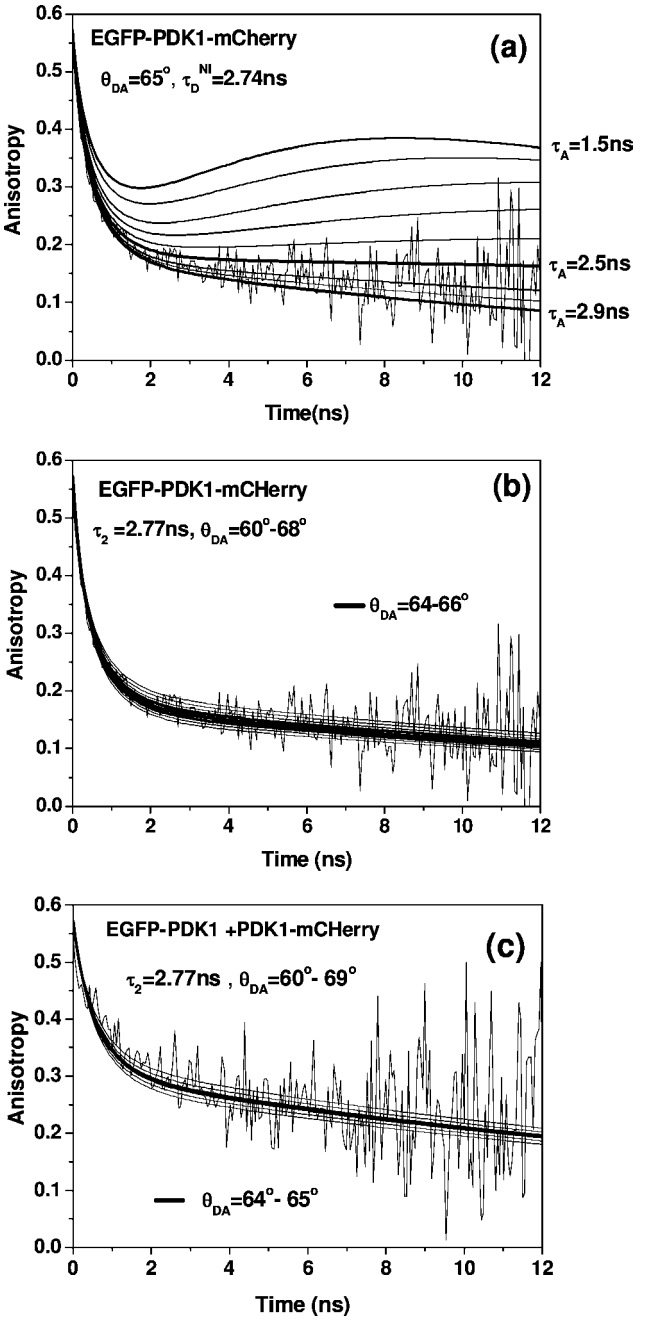

Figure 6. (a) Model anisotropy decays showing the sensitivity of the composite anisotropy for EGFP-PDK1-mCherry to the lifetime of FRET excited mCherry for an interchromophore angle of 65°. (b,c) Model anisotropy decays for EGFP-PDK1-mCherry EGFP-PDK1+PDK1-mCherry and assuming FRET takes place exclusively to the longer lived 2.77 ns state of mCherry for a range of donor−acceptor angles.

FRET restricted to the 2.77 ns state are shown in Figure 6b and c for EGFP-PDK1-mCherry and EGFP-PDK1+PDK1-mCherry, respectively, and both are well described by interchromophore angles around 65°.

In an isotropic medium, single-photon excitation is independent of the molecular frame orientations of the participating transition dipole moments. FRET photoselection, however, is firmly based on such factors, which are encapsulated in the κ^2 orientation parameter.[9,10] For a given θ_{DA}, a range of κ^2 values are possible (see Supporting Information Appendix 6); however, given the limited local rotational diffusion of both fluorophores (Table S1 and Figure S5, Supporting Information), the same degree of excited-state population in sensitized mCherry emission (i.e., the fast and slow lifetime weightings in Figure 4b) should not necessarily be expected.

dx.doi.org/10.1021/ja312230b | J. Am. Chem. Soc. 2013, 135, 7883−7890

A slow transfer rate from EGFP to the shorter lived state in mCherry should give rise to fluorescence that is characterized by an apparent rise time equal to the fluorescence lifetime of the shorter lived state (1.47 ns) and a decay with a lifetime no greater than that of the interacting EGFP donor (see Appendix 5, Supporting Information).[7] The absence of such a feature in the in-growth of the sensitized mCherry fluorescence together with the anisotropy results of Figures 5 and 6 strongly indicate that this energy transfer route is effectively closed in the PDK1 dimer. We therefore conclude that FRET takes place exclusively between the shorter lived (2.43 ns) excited state of EGFP and the longer lived (2.77 ns) state of mCherry. In this light, the low interacting fraction we observe, ca. 6% in EGFP-PDK1-mCherry, can be explained; one-half the available excited EGFP population does not undergo FRET, and only ca. 16% the available mCherry population can act as acceptors. Measurements of the degree of in vitro PDK1 dimerization using size exclusion chromatography yielded a high interacting fraction (ca. 70%).[17] Given the reduction in the possible interacting donor and acceptor states, the optically active interacting fraction underestimates the true interacting fraction by a factor of ca. 13.

Our observations differ from recent work by Visser and coworkers who have studied intramolecular FRET in an EGFP-L_6-mCherry construct where the two chromophores are linked by a 6 amino acid chain.[21,23] In recombinant protein samples, they detect three rise times, 0.78 ns, 0.23 ns, and 72 ps, together with an mCherry fluorescence decay of 1.89 ns.[21] In live cells, global analysis yields a rise time of 0.54 ns and an average (acceptor window) lifetime of ca. 2 ns.[23] The low interacting EGFP fraction measured in both experiments is attributed to background contamination by nonmatured and noninteracting mCherry.[21,23] In both experiments, the dominant FRET acceptor is the shorter lived state of mCherry.

The multiplicity of rise times is attributed to the flexibility of the linker, which would result in a distribution of relative orientations and distances between EGFP and mCherry.[21] We observe little local (flexible) motion of EGFP and mCherry when fused to PDK1 (Table S1 and Figure S4, Supporting Information), and our observation of restricted FRET between the two fluorophores would indicate that orientational constraints in the PDK1 dimer are the cause of the state selection we observe. Unequal resonance transfer between EGFP and two acceptor states of mCherry has recently been observed in single molecule and time-resolved FRET experiments by Wu et al.[24] In their work, EGFP and mCherry were attached to a range of fusion proteins with presumably far less orientational freedom than the amino acid linked construct.[21,23] It appears that the donor–acceptor environment may play a critical role in the extent to which FRET can take place between EGFP and mCherry.

Chromophore Orientation and Differential State Selection in FRET. Having determined θ_{DA}, we can estimate κ^2 and the interchromophore separation by both analytical methods and computer simulation (see Appendix 6, Supporting Information). A lower limit on κ^2 is provided by the minimum distance that the two fluorescent chromophores can approach (ca. 3 nm) corresponding to direct contact between EGFP and mCherry. The mechanism for the reduced quantum yield (lifetime shortening) in fluorescent proteins such as mCherry is attributed to twisting of the chromophore from the planar structure found in wild-type GFP.[25] Thus, the short-lived state in mCherry may correspond to a rotated acceptor dipole. To test this proposition, we examined κ^2 values for two donor–acceptor dipole geometries, far from and close to planar. The populations of interacting and noninteracting EGFP and mCherry should be identical in terms of the molecular frame orientation of the fluorescent proteins within the PDK1 dimer, and the in-plane angle θ_D in eq SI-33 and Figure S7 should be common to both. If θ_D is close to the in-plane acceptor angles, θ_{A1} and θ_{A2}, κ^2 (eq SI-33) is given by:

$$\kappa^2 = (\sin^2\theta\cos\phi - 2\cos^2\theta)^2 \quad (9)$$

Variations in κ^2 with θ for transition dipole orientations in a far from and close to coplanar interaction geometry are shown in Figure 7. In the noncoplanar geometry, it is possible to find a θ

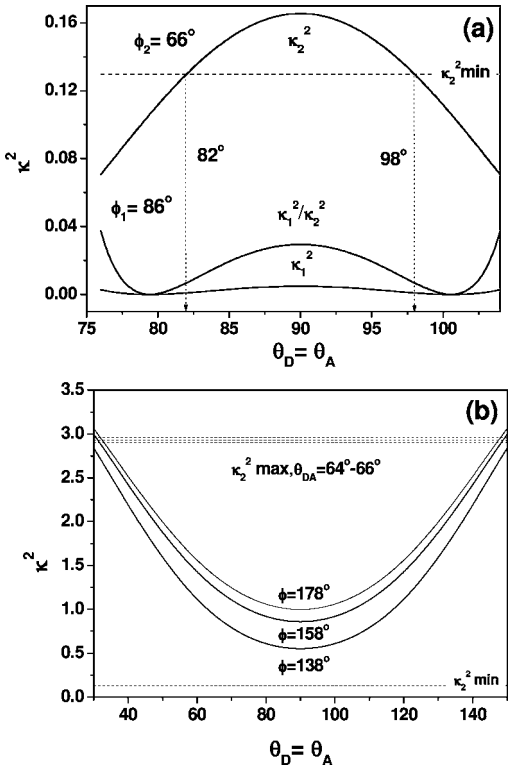

Figure 7. (a) Variation in κ^2 with θ ($\theta_D = \theta_A$) for two different acceptor transition dipole orientations in mCherry ($\phi_1 = 86°$ and $\phi_2 = 66°$) in a far from planar interaction geometry with $\theta_{DA} = 65 \pm 1°$. Between $\theta = 82°$ and $\theta = 98°$, κ_1^2 is sufficiently low to yield a κ^2 ratio between 6.8×10^{-3} and 2.94×10^{-2}, while κ_2^2 is within the range corresponding to the observed FRET rise time for EGFP-PDK1-mCherry. (b) Variation in κ^2 in a close to planar geometry; a ±20° change in ϕ does not give sufficient variation in κ^2 to allow for differential (molecular frame) orientational photoselection.

range (allowed by θ_{DA}, e.g., $65 \pm 1°$) in which a change in the interplane angle ϕ of 20° gives rise to κ_2^2 values that correspond to a physically reasonable donor–acceptor separation, and a κ_1^2/κ_2^2 value that would correspond to a low FRET efficiency for transfer to the rotated acceptor dipole. In the near coplanar geometry, variation of ϕ in the allowed θ range does not lead to differential photoselection between the two transition dipoles. This simplified analysis indicates that if molecular frame orientational photoselection is the mechanism for differential FRET between EGFP and mCherry, then the geometry between the chromophores cannot be near to planar. The lower values of κ_2^2 that this analysis points to would indicate that the chromophore separation is much closer to the

dx.doi.org/10.1021/ja312230b | J. Am. Chem. Soc. 2013, 135, 7883–7890

mimimum approach of 3 nm than is predicted by computer modeling of the κ^2 distribution (see Figure S7).

CONCLUSIONS

We have shown that the combination of spectrally resolved fluorescence intensity and anisotropy measurements is a significant help in unraveling the FRET dynamics of an inhomogeneous system. For FRET between EGFP and mCherry, the observation of rapid FRET depolarization that is maintained in the presence of a large background of high anisotropy noninteracting donors is only possible when the lifetimes of the FRET accessed states in mCherry are close to those of the noninteracting EGFP population. Dipole−dipole transfer has the same selection rules as single-photon excitation;[7,22] however, in FRET, photoselection takes place in the molecular frame of reference where donor and acceptor transition dipole moments are not necessarily isotropically distributed. For single-photon excitation in an isotropic medium, transition rates are independent of polarization;[26] all states in mCherry are accessed on the basis of their relative ground-state populations and individual transition moment strengths. Fluorescence decays in EGFP and mCherry are biexponential; the minor component of mCherry fluorescence with a lifetime in the region of 2.77 ns is the state accessed by FRET from the shorter lived excited state of EGFP. The effect of this restriction from four possible FRET pathways (2 donor states in EGFP and 2 acceptor states in mCherry) to one greatly reduces the degree of FRET that is observed and as discussed above appears to be dependent on the fluorescent protein environment. We are at present investigating continuous wave stimulated emission depletion in EGFP and mCherry as a means of characterizing the radiative decay rates and relative dipole strengths of the two states in each system, and the results of this work will be reported shortly and should help clarify more fully the origin of the strongly restricted FRET that we have observed in this study.

Restricted state selection in fluorescent protein FRET has significant consequences for FRET experiments where such restrictions (if present) are not revealed. The low degree of FRET that results would lead to erroneous measurements of interacting fractions and FRET efficiencies and consequently affect the broad interpretation of experimental results. Our results point to the value of combining fluorescence intensity and anisotropy measurements as a means of more fully characterizing FRET in heterogeneous systems.

ASSOCIATED CONTENT

Supporting Information

Six appendices, seven figures, two tables, and a program. This material is available free of charge via the Internet at http://pubs.acs.org.

AUTHOR INFORMATION

Corresponding Author

a.bain@ucl.ac.uk; banafshe.larijani@cancer.org.uk

Present Address

[§]T.A.M.: Mechanobiology Institute, National University of Singapore, 5A Engineering Drive 1, Singapore 117411, Singapore

Notes

The authors declare no competing financial interest.

ACKNOWLEDGMENTS

We are grateful to EPSRC, UCL, and Cancer Research UK for funding and a Ph.D. studentship for Thomas Masters via the CoMPLEX Doctoral Training Centre at UCL. We gladly acknowledge the help of Sara Kisakye-Nambozo and Svend Kjaer (Cancer Research UK) with the baculovirus work and protein purification. We thank You Li for assistance with illustrations.

REFERENCES

(1) Stryer, L. *Annu. Rev. Biochem.* **1978**, *47*, 819−846.
(2) Selvin, P. R. *Nat. Struct. Biol.* **2000**, *7*, 730−734.
(3) Masters, T. J.; Calleja, V.; Armoogum, D. A.; Marsh, R. J.; Applebee, C. J.; Laguerre, M.; Bain, A. J.; Larijani, B. *Sci. Signaling* **2010**, *3*, ra78.
(4) Tanaka, F.; Mataga, N. *Photochem. Photobiol.* **1979**, *29*, 1091−1097.
(5) Visser, N. V.; Borst, J. W.; Hink, M. A; van Hoek, A.; Visser, A. J. *Biophys. Chem.* **2005**, *116*, 207−212.
(6) Borst, J. W.; Laptenok, S. P.; Westphal, A. H.; Kuhnemuth, R.; Hornen, H.; Visser, N. V.; Kalinin, S.; Aker, J.; van Hoek, A.; Seidel, C. A.; Visser, A. J. *Biophys. J.* **2008**, *95*, 5399−5411.
(7) Valeur, B. *Molecular Fluorescence.: Principles and Applications*; Wiley-VCH: Weinheim, 2002.
(8) van der Meer, B. W. *J. Biotechnol.* **2002**, *82*, 181−196.
(9) Dale, R. E.; Eisinger, J. *Biopolymers* **1974**, *13*, 1573−1605.
(10) Dale, R. E.; Eisinger, J.; Blumberg, W. E. *Biophys. J.* **1979**, *26*, 161−193.
(11) Ludescher, R. D.; Peting, L.; Hudson, S.; Hudson, B. *Biophys. Chem.* **1987**, *28*, 59−75.
(12) Ruggiero, A.; Hudson, B. *Biophys. J.* **1989**, *55*, 1111−1124.
(13) Carver, T. E.; Hochstrasser, R. A.; Millar, D. P. *Proc. Natl. Acad. Sci. U.S.A.* **1994**, *91*, 10670−10674.
(14) Ko, C. W.; Wei, Z.; Marsh, R. J.; Armoogum, D. A.; Nicolaou, N.; Bain, A. J.; Zhou, A.; Ying, L. *Mol. BioSyst.* **2009**, *5*, 1025−1031.
(15) Drobizhev, M.; Tillo, S.; Makarov, N. S.; Hughes, T. E.; Rebane, A. *J. Phys. Chem. B* **2009**, *113*, 855−859.
(16) Drobishev, M. 2010, personal communication.
(17) Masters, T. A. Ph.D. Thesis. UCL, London, 2009.
(18) Wan, C.; Johnson, C. K. *Chem. Phys.* **1994**, 513−31.
(19) Heikal, A. A.; Hess, S. T.; Webb, W. W. *Chem. Phys.* **2001**, *274*, 37−45.
(20) Hess, S. T.; Sheets, E. D.; Wagenknecht-Wiesener, A.; Heikal, A. A. *Biophys. J.* **2003**, *85*, 2566−2580.
(21) Visser, A. J. W. G.; Laptenok, S. P.; Visser, N. V.; van Hoek, A.; Birch, D. J. S.; Brochon, J.-C.; Borst, J. W. *Eur. Biophys. J.* **2010**, *39*, 241−253.
(22) Andrews, D. L., Demidov, A. A., Eds. *Resonance Energy Transfer*; Wiley: New York, 1999.
(23) Laptenok, S. P.; Borst, J. W.; Mullen, K. M.; van Stokkum, I. H. M.; Visser, A. J. W. G.; van Amerongen, H. *Phys. Chem. Chem. Phys.* **2010**, *12*, 7593−7602.
(24) Wu, B.; Chen, Y.; Müller, J. D. *Biophys. J.* **2009**, *96*, 2391−2404.
(25) Shu, X.; Shaner, N. C.; Yarbrough, C. A.; Tsein, R. Y.; Remington, S. *Biochemistry* **2006**, *45*, 9639−9647.
(26) Brink, D. M.; Satchler, G. R. *Angular Momentum*, 3rd ed.; Clarendon Press: Oxford, 1993.